Comparing efficiency and accuracy of the kinoform and the helical axicon as Bessel–Gauss beam generators

Victor Arrizón,[1,*] Ulises Ruiz,[1] Dilia Aguirre-Olivas,[1] David Sánchez-de-la-Llave,[1] and Andrey S. Ostrovsky[2]

[1]*Instituto Nacional de Astrofísica, Óptica y Electrónica, Puebla 72000, Mexico*
[2]*Facultad de Ciencias Físico Matemáticas, Benemérita Universidad Autónoma de Puebla, Puebla 72000, Mexico*
**Corresponding author: arrizon@inaoep.mx*

Received September 12, 2013; revised December 22, 2013; accepted December 24, 2013; posted December 24, 2013 (Doc. ID 197644); published February 5, 2014

We compare two phase optical elements that are employed to generate approximate Bessel–Gauss beams of arbitrary order. These elements are the helical axicon (HA) and the kinoform of the desired Bessel–Gauss beam. The HA generates a Bessel beam (BB) by free propagation, and the kinoform is employed in a Fourier spatial filtering optical setup. As the main result, it is obtained that the error in the BBs generated with the kinoform is smaller than the error in the beams obtained with the HA. On the other hand, it is obtained that the efficiencies of the methods are approximately 1.0 (HA) and 0.7 (kinoform).

OCIS codes: (350.7420) Waves; (090.1760) Computer holography; (090.1970) Diffractive optics; (050.4865) Optical vortices.
http://dx.doi.org/10.1364/JOSAA.31.000487

1. INTRODUCTION

In recent years the study of Bessel beams (BBs) has become an attractive topic of research in optics [1–3]. The orbital angular momentum and the invariance under propagation of BBs have propitiated their application in nonlinear optical guides [4] and optical tweezers [5–7], among other fields. The BBs have been generated with different techniques. The method proposed by Durnin *et al.* [8], based on the Fourier transform of a narrow annular slit, allows the generation of a zero order BB. Later on, a BB of arbitrary order was generated by encoding a helical axicon (HA) using a computer-generated hologram [9,10]. Another approach for obtaining an arbitrary BB requires the generation of a high-order Laguerre–Gauss beam that is employed to illuminate an axicon [11]. An arbitrary optical field, and a BB as a particular case, can be generated employing general-purpose synthetic phase holograms (SPHs) [12–14]. The drawback of these SPHs is their relatively low efficiency.

The efficiency in the generation of a BB with a HA is increased by implementing this optical element with a phase spatial light modulator (SLM) [15,16]. The HA, whose phase structure generates convergent conical waves, produces high-order BBs by free propagation, without the necessity of additional components. Another phase optical element that allows the generation of a BB with relatively high efficiency is the so-called Bessel beam kinoform (BBK), whose phase modulation is the phase of the BB itself [16–18]. This optical element has been employed in a 4-f optical setup, with a binary spatial filter (SF), for generating an arbitrary order BB [17].

Considering that the natural mode of a laser source is a Gaussian beam, it is usual and convenient to consider the generation of Bessel–Gauss beams (BGBs). A BGB is obtained by employing a Gaussian beam as the illuminating source in the setups that employ HAs and BBKs to generate a BB. In the performance evaluation of HAs and BBKs it is important to consider the accuracy of the BGBs generated by these optical elements. A low efficiency in the generation of a BGB can be overcome by increasing the power of the light source. However, errors in the intensity and phase profiles of the BGBs cannot be easily corrected. An accurate BGB is required, e.g., in a laser resonator, for a good mode–matching of the beam to the resonator cavity [19].

In the present study we analyze and evaluate the performances of HAs and BBKs, as BGB generators. In this analysis we consider the efficiencies of both methods and the accuracy of the intensity profiles and phases of the approximate generated BGBs. The accuracy is evaluated by the root mean square deviation (RMSD), between the synthesized BGBs and their corresponding analytic BGBs.

In order to make the reading of the manuscript self-contained, in Section 2 we review the basic theory and the general aspects of the setups that employ HAs and BBKs to generate a BGB. In Section 3 we evaluate numerically the efficiency and the accuracy of the two methods. The experimental implementation of the two methods is illustrated in Section 4. Conclusions and final remarks are presented in Section 5.

2. PHASE OPTICAL ELEMENTS

The complex amplitude of the desired qth order BGB is expressed as

$$b(r,\theta) = J_q(2\pi r/r_0)\exp(-r^2/w^2)\exp[iq\theta], \tag{1}$$

where (r, θ) are polar coordinates, r_0 is the asymptotic radial period, w is the waist of the Gaussian modulation, and J_q is the qth order Bessel function. Let us consider an optical element with transmittance

$$t(r,\theta) = f_1(r)\exp(iq\theta). \tag{2}$$

This function can be expressed, within the radial domain $[0, R]$, by the Fourier Bessel series

$$t(r,\theta) = \sum_{n=1}^{\infty} b_n J_q(\lambda_n r/R)\exp(iq\theta), \tag{3}$$

where λ_n is the nth positive root of $J_q(x)$, and

$$b_n = \frac{2}{J_{q+1}^2(\lambda_n)}\int_0^1 x f_1(Rx) J_q(\lambda_n x)\mathrm{d}x. \tag{4}$$

When the optical element $t(r,\theta)$ is illuminated by the Gaussian beam $\exp(-r^2/w^2)$, the field transmitted is formed, according to Eq. (3), by a series of qth order BGBs with radial frequencies proportional to the roots λ_n. Therefore, the optical device $t(r,\theta)$ in Eq. (2) is potentially useful for the generation of BGBs. The transmittances of the HA and the BBK are particular forms of the function $t(r,\theta)$. The setups where the HA and the BBK have been employed to generate a BGB, are next briefly reviewed.

A. Bessel Beam Kinoform

The BBK transmittance is given by Eq. (2) with radial modulation

$$f_1(r) = \mathrm{sgn}[J_q(2\pi r/r_0)]\mathrm{circ}(r/R), \tag{5}$$

where sgn denotes the signum function and $\mathrm{circ}(r/R)$ is a circular pupil of radius R that bounds the device. Now, it is assumed that the relation $2\pi R/r_0 = \lambda_m$ is fulfilled for the root λ_m. Thus, the mth order BGB transmitted by the BBK, when it is illuminated by the Gaussian field $\exp(-r^2/w^2)$, corresponds to the qth order BGB given in Eq. (1), with weighting factor b_m. Moreover, the integrand in Eq. (4) for $n = m$ becomes positive, providing a relatively high value for the coefficient b_m. Since the Fourier spectra of these multiple BGBs is formed by concentric rings of different radii, the mth order BGB can be isolated in the Fourier domain of the BBK by applying an annular pupil.

To illustrate the general features of the method we consider the BBK of order $q = 1$ assuming that $m = 10$ and that the waist of the Gaussian beam is $w = R$. The BBK phase and the numerically computed Fourier spectrum modulus of the transmitted field are depicted in Figs. 1(a) and 1(b). In Fig. 1(b) the brightest ring is the Fourier spectrum of the first order BGB that corresponds to the index $m = 10$. The spectrum filtering is made by an annular pupil that only transmits the light of the brightest ring. The inner and outer radii of this pupil coincide with the dark zones that limit the brightest ring. The field transmitted by the filter, shown in Fig. 1(c), is Fourier transformed to generate the desired BGB. The normalized intensity of the numerically generated BGB in this case is partially displayed in Fig. 1(d).

B. Helical Axicon

The HA transmittance is given by Eq. (2) with radial modulation

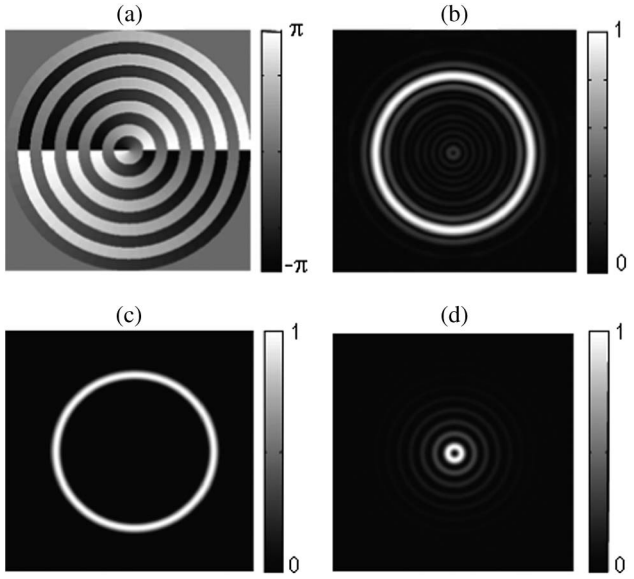

Fig. 1. (a) Phase modulation of the first order BBK, (b) Fourier spectrum modulus of the BBK when it is illuminated by the Gaussian beam $\exp(-r^2/R^2)$, (c) BBK Fourier spectrum after the application of the annular SF, and (d) intensity of the numerically generated BGB.

$$f_1(r) = \exp(-i2\pi r/r_0)\mathrm{circ}(r/R). \tag{6}$$

A rough picture of the spatial distribution of the light transmitted by the HA, shown in Fig. 2, is obtained from geometrical ray tracing, considering only the radial phase of the element. The radial phase of the HA deviates incident rays by an angle $\psi = \mathrm{asin}(\lambda/r_0)$, where λ is the light wavelength. Thus, it can be shown that the largest section of interference of the conic beams, at the center of the dark gray zone in Fig. 2, occurs at the distance $z = z_c = R(r_0^2 - \lambda^2)^{1/2}/(2\lambda)$. In Section 3, the approximate BGBs generated by HAs are computed and evaluated at the plane $z = z_c$.

The field transmitted by the HA is formed, according to Eq. (3), by multiple qth order BGBs with different spatial frequencies and different amplitudes b_n. Assuming that the relation $2\pi R/r_0 = \lambda_m$ is fulfilled for the root λ_m, the mth order BGB transmitted by the HA corresponds to the qth order BGB given in Eq. (1), with weighting factor b_m.

We compute the optical field freely propagated from the HA using the angular spectrum method [20]. Considering that the HA, whose transmittance is given by Eq. (2), is illuminated by a Gaussian field $\exp(-r^2/w^2)$, the Fourier transform of the transmitted field is given by $\exp(iq\phi)\ F_1(\rho)$, where $F_1(\rho)$ is the qth order Hankel transform of $f_1(r)\exp(-r^2/w^2)$. The optical field propagated to the plane located at a distance z_c from the HA is expressed as

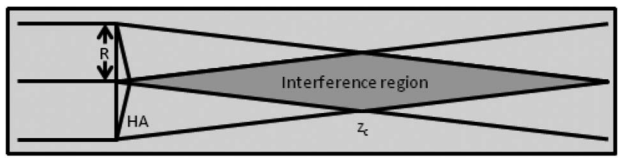

Fig. 2. Interference region (dark gray), where a BGB is approximately generated by a HA and plane $z = z_c$ of maximum interference area.

$$g(r,\theta) = \exp(iq\theta) g_1(r), \tag{7}$$

where $g_1(r)$ is the inverse Hankel transform of the product $F_1(\rho)\ \exp[ikz_c(1-\lambda^2\rho^2)^{1/2})]$ and $k = 2\pi/\lambda$. This method is applied in Section 3 to compute and evaluate the approximate BGBs generated with HAs.

3. PERFORMANCE OF THE TECHNIQUES

Next, we analyze the performance of HAs and BBKs as BGB generators. It is assumed that the radial domain $[0, R]$ of these optical elements covers m roots of the radial modulation $J_q(2\pi r/r_0)$ of the BGB to be generated. We also assume that the optical elements are illuminated by a Gaussian beam with amplitude $\exp(-r^2/w^2)$. Although the width of the Gaussian beam can be arbitrarily chosen for numerical simulations, we adopt the reasonable value $w = R$. For this width the pupil of the optical elements transmits approximately 86.5% of the power of the Gaussian beam.

A. Efficiency

The efficiency of a BBK and a HA in the generation of a BGB is the optical power of this generated beam, normalized by the optical power transmitted (or reflected) by the optical element. A HA generates an approximate BGB with an efficiency close to 1.0. The reason is that, as suggested in Fig. 2, the whole optical field transmitted by the HA forms the conical waves that interfere to generate the BGB. In the case of the BBK, the BGB is obtained from the light transmitted by the binary SF applied to the brightest ring in the BBK Fourier spectrum (Fig. 1). In this case the efficiency can be computed by the power of the light transmitted by the binary filter, normalized by the power of the complete Fourier spectrum of the BBK. As illustrative cases we compute the efficiencies of BBKs employed to generate BGBs of orders $q = 0$ to 10, with $m = 10$ and $m = 20$. The obtained efficiencies, shown in Fig. 3, are similar to the ones obtained for many other values of q and m.

B. Accuracy

Considering the transmittances of the BBK and the HA, and the optical setups employed to generate an approximate BGB with these optical elements, the complex amplitudes of the generated beams can be expressed by the function $\exp(iq\theta)\ g_1(r)$, as shown in Eq. (7). On the other hand the complex amplitude of the exact qth order BGB [Eq. (1)] has the form $b(r,\theta) = \exp(iq\theta) b_1(r)$, where $b_1(r) = J_q(2\pi r/r_0)\exp(-r^2/w^2)$. Thus, in the evaluation of an approximate BGB generated with any of the discussed methods, we only need to compare the radial modulations $g_1(r)$ and $b_1(r)$. For both optical elements the generated BGB is computed and evaluated for r in the interval $[0, R/2]$ that corresponds to the section of interference at the plane $z = z_c$ (Fig. 2). The RMSD of $g_1(r)$ respect to $b_1(r)$ is given by

$$D = \left[A^{-1}\int_0^{R/2} |b_1(r) - \alpha\exp(i\beta) g_1(r)|^2 dr\right]^{1/2}, \tag{8}$$

where $\alpha\exp(i\beta)$ is a complex constant for the best fitting of the complex fields $g_1(r)$ and $b_1(r)$, and $A = R/2$ is the length of the domain where the deviation is computed. The values of α and β are obtained from the conditions $\partial D/\partial\alpha = 0$ and $\partial D/\partial\beta = 0$.

Representative RMSDs for the BGBs generated using the two methods are shown in Fig. 4. These results correspond to BGB orders $q = 0$ to 10 with $m = 10$ and $m = 20$. An important result is that the method employing BBKs provides significantly lower RMSDs than the approach using HAs. The RMSD in Eq. (8) takes into account both the phase and the intensity errors of the generated BGB. In the considered cases we computed the fitting parameters α and β after the normalization of $b_1(r)$.

Representative phase and intensity profiles of the approximate first-order BGBs generated with the two methods are displayed in Figs. 5 and 6. The function $g_1(r)$ considered in each case is multiplied by the fitting factor $\alpha\exp(i\beta)$. The number of roots of the BGB radial modulation in the element's radius R for the discussed cases are respectively $m = 10$ and $m = 20$. The radial coordinate r in the interval $[0, R/2]$ of the plots appears normalized by the asymptotic period r_0. For reference, the transverse normalized intensities and the

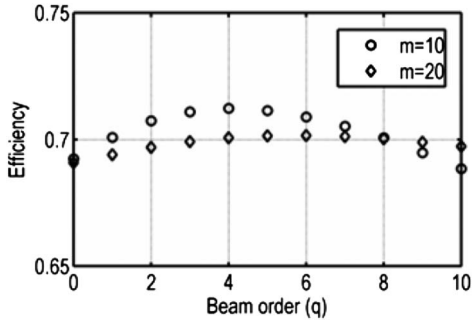

Fig. 3. Efficiencies of BBKs with $m = 10$ and $m = 20$ in generation of BGBs of orders $q = 0$ to 10.

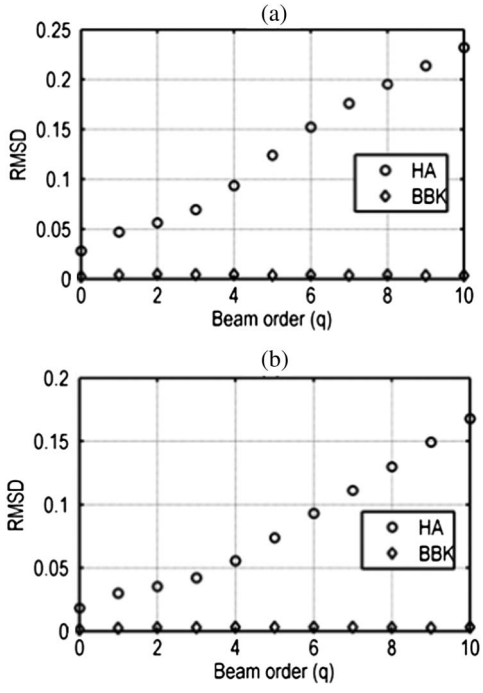

Fig. 4. RMSDs of transverse profiles of BGB of orders $q = 0$ to 10 generated by HAs and BBKs, employing pupils with (a) $m = 10$ and (b) $m = 20$.

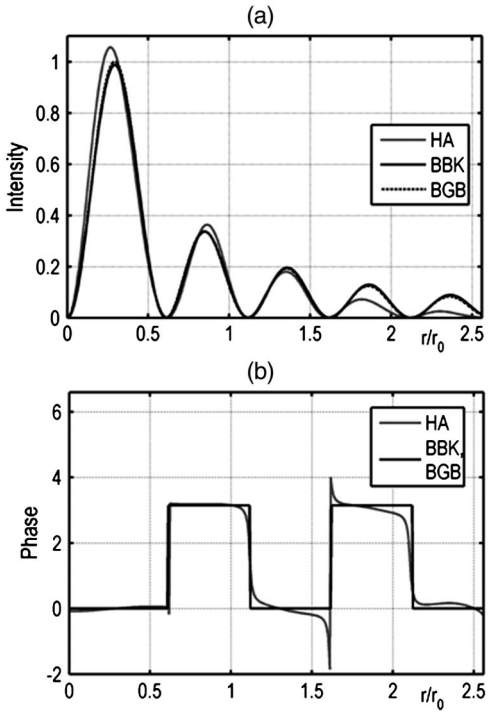

Fig. 5. (a) Transverse phase profiles and (b) phases of a theoretical BGB and of the approximate BGBs generated by a HA and a BBK with $m = 10$.

phases of the theoretical BGBs are also presented in each case.

In some applications it is only important to consider the intensity profiles of the generated beams. In this case a convenient evaluation of the beams is provided by the normalized

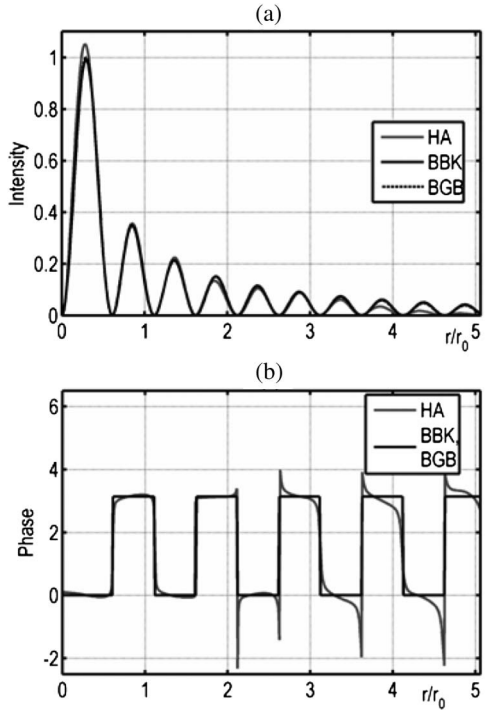

Fig. 6. (a) Transverse intensity profiles and (b) phases of a theoretical BGB and of the approximate BGBs generated by a HA and a BBK with $m = 20$.

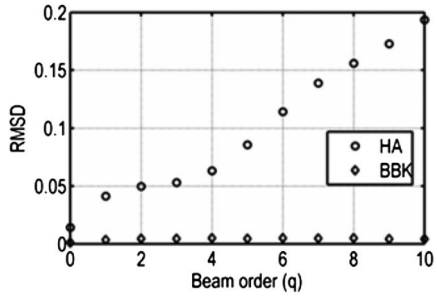

Fig. 7. RMSDs of transverse intensity profiles of BGB of orders $q = 0$ to 10 generated by HAs and BBKs, employing a pupil with $m = 10$.

RMSD between $I_g(r)$ and $I_b(r)$, which correspond to the intensities of the fields $g_1(r)$ and $b_1(r)$, respectively. Such RMSD is

$$D = \left[A^{-1}\int_0^{R/2} |I_b(r) - \alpha I_g(r)|^2 \mathrm{d}r\right]^{1/2}, \tag{9}$$

where α is a scaling constant for the best fitting of the functions $I_g(r)$ and $I_b(r)$, obtained from the condition $\partial D/\partial\alpha = 0$. The RMSD formula in Eq. (9) provides lower values than the RMSD in Eq. (8) because it ignores phase errors. Examples of the intensity-only RMSDs, presented in Fig. 7, correspond to the BGBs of orders $q = 0$ to 10, with $m = 10$.

4. EXPERIMENTAL BEAM SYNTHESIS EXAMPLES

The optical setup where BBKs are employed to generate BGBs, depicted in Fig. 8, was previously described in the cited [17]. In this setup, the Gaussian beam of a He–Ne laser is expanded (by the beam expander BE) to illuminate a reflective type phase SLM (from HOLOEYE Photonics AG). The light reflected by the BBK, which is displayed in the SLM, is the input of a 4-f optical system, formed by two lenses (L_1 and L_2) and an annular SF. The Lens L_1 projects the BBK Fourier transform to the SF plane. The brightest ring in this Fourier spectrum is transmitted by the SF, and Fourier transformed again (by lens L_2) to generate the BGB, which is detected by a CCD camera. The setup for a HA is similar to that in Fig. 8, but in this case the components L1, L2, and SF are removed, and the sensor of the CCD is placed at a distance $z = z_c$ from the SLM, where the maximum interference area of the HA conic waves appears.

We implemented and displayed in the SLM a HA and a BBK for the generation of a first order BGB, bounded by a pupil that covers 10 roots of the function $J_1(2\pi r/r_0)$. The Gaussian beam is conditioned to show a width w approximately equal to the radius R of the pupil limiting the displayed optical elements. To avoid light reflected without modulation in the optical axis of the setup, the transmittances of the BBK and HA are multiplied by a linear phase carrier, which allows

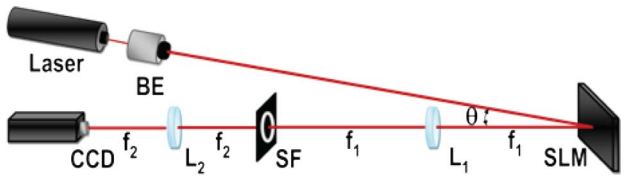

Fig. 8. Optical setup for the experimental generation of a BGB employing a BBK.

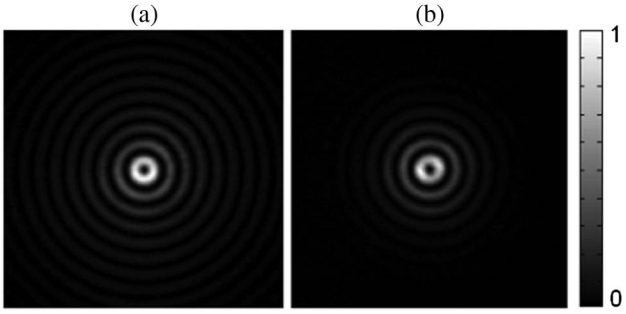

Fig. 9. Intensities of the first order BGBs experimentally generated by (a) a BBK and (b) a HA. The limiting pupils covers 10 roots of the radial modulation $J_1(2\pi r/r_0)$.

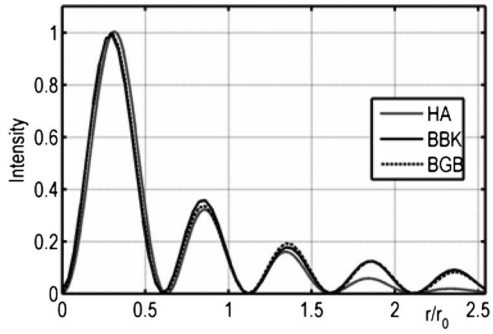

Fig. 10. Transverse intensity profiles of the experimental BGBs displayed in Fig. 9 and of the corresponding theoretic BGB.

an appropriate off–axis generation of the BGB. The phase curvature of the Gaussian beam illuminating the SLM is measured and compensated in the phase functions displayed in this device. The intensities of the experimentally generated first-order BGBs are shown in Fig. 9 and the normalized transverse intensity profiles of these beams are depicted in Fig. 10. For comparison, the intensity profile of the desired BGB is also presented in Fig. 10. The displayed profiles have been corrected by the fitting factor α, obtained from the relation $\partial D/\partial\alpha = 0$, for the deviation D expressed in Eq. (9). The intensity profiles of the experimentally generated fields approximately correspond to the numerically calculated intensity profiles displayed in Fig. 5(a). The RMSDs of the experimental intensity profiles, computed with Eq. (9), are approximately 0.008 for the BBK and 0.05 for the HA. These RMSDs are a little larger than the ones obtained numerically for the HA and the BBK with the parameters considered in the experiment, which correspond to the case $q = 1$ in Fig. 7.

5. FINAL REMARKS AND CONCLUSIONS

We have evaluated and compared the intensity and phase profiles of BGBs generated with HAs and BBKs. The results proved that the BBKs allow the generation of BGBs more accurately than the HAs. The accuracy is measured by the RMSD of the transverse profiles of the fields generated by the two considered optical devices. Such deviation is measured respect to the desired BGB. In a first case the RMSD considers both the phase and intensity errors in the generated fields. In the second case the RMSD takes into account only the intensity profiles.

When any of the considered optical elements, the BBK and the HA, is illuminated by a Gaussian beam, the transmitted field is formed by multiple BGBs with different radial frequencies. In the case of the BBK, the employed spatial filtering setup allows the isolation of a single BGB, with the desired frequency. Therefore the generated BGB in this case shows a very low RMSD. A drawback of this method is the loss of approximately 30% of light power in the filtering step.

In the case of the HA, several of the BGBs transmitted by the optical element partially interfere in the propagation space to form an approximate version of the desired BGB. This explains the higher RMSD for the HA case compared to the BBK case, and thus, the decreased accuracy. The positive counterpart is that the efficiency in this case is close to 1.0.

If the application of a BGB requires a high precision in its intensity profile and phase it is preferable the use of a BBK (and its required setup) to generate it. However, if the application does not require a highly precise BGB it can be generated using a HA. The advantages in this case are the relatively high-energy throughput of the approach and the simplicity of the required setup.

REFERENCES

1. D. McGloin and K. Dholakia, "Bessel beams: diffraction in a new light," Contemp. Phys. **46**, 15–28 (2005).
2. M. Padgett and R. Bowman, "Tweezers with a twist," Nat. Photonics **5**, 343–348 (2011).
3. A. Dudley, M. Lavery, M. Padgett, and A. Forbes, "Unraveling Bessel beams," Opt. Photon. News **24**(6), 22–29 (2013).
4. J. Arlt, K. Dholakia, J. Soneson, and E. M. Wright, "Optical dipole traps and atomic waveguides based on Bessel light beams," Phys. Rev. A **63**, 063602 (2001).
5. V. Garcés-Chávez, D. McGloin, H. Melville, W. Sibbett, and K. Dholakia, "Simultaneous micromanipulation in multiple planes using self-reconstructing light beam," Nature **419**, 145–147 (2002).
6. J. E. Molloy, K. Dholakia, and M. Padgett, "Optical tweezers in a new light," J. Mod. Opt. **50**, 1501–1507 (2003).
7. T. Cizmár, V. Kllárová, X. Tsampoula, F. Gunn-Moore, W. Sibbett, Z. Bouchal, and K. Dholakia, "Generation of multiple Bessel beams for a biophotonics workstation," Opt. Express **16**, 14024–14035 (2008).
8. J. Durnin, J. J. Miceli, Jr., and J. H. Eberly, "Diffraction-free beams," Phys. Rev. Lett. **58**, 1499–1501 (1987).
9. A. Vassara, J. Turunen, and A. T. Friberg, "Realization of general nondiffracting beams with computer-generated holograms," J. Opt. Soc. Am. A **6**, 1748–1754 (1989).
10. C. Paterson and R. Smith, "Higher-order Bessel waves produced by axicon-type computer-generated holograms," Opt. Commun. **124**, 121–130 (1996).
11. J. Arlt and K. Dholakia, "Generation of high-order Bessel beams by use of an axicon," Opt. Commun. **177**, 297–301 (2000).
12. V. Arrizón, U. Ruiz, R. Carrada, and L. A. González, "Pixelated phase computer holograms for the accurate encoding of scalar complex fields," J. Opt. Soc. Am. A **24**, 3500–3507 (2007).
13. T. Ando, Y. Ohtake, N. Matsumoto, T. Inoue, and N. Fukuchi, "Mode purities of Laguerre–Gaussian beams generated via complex-amplitude modulation using phase-only spatial light modulators," Opt. Lett. **34**, 34–36 (2009).
14. J. A. Rodrigo, T. Alieva, A. Cámara, Ó. Martínez-Matos, P. Cheben, and M. L. Calvo, "Characterization of holographically generated beams via phase retrieval based on Wigner distribution projections," Opt. Express **19**, 6064–6077 (2011).
15. N. Chattrapiban, E. A. Rogers, D. Cofield, W. T. Hill III, and R. Roy, "Generation of nondiffracting Bessel beams by

use of a spatial light modulator," Opt. Lett. **28**, 2183–2185 (2003).
16. M. McLaren, J. Romero, M. J. Padgett, F. S. Roux, and A. Forbes, "Two-photon optics of Bessel-Gaussian modes," http://arxiv.org/abs/1306.2767.
17. V. Arrizón, D. Sánchez-de-la-Llave, U. Ruiz, and G. Méndez, "Efficient generation of an arbitrary nondiffracting Bessel beam employing its phase modulation," Opt. Lett. **34**, 1456–1458 (2009).
18. M. McLaren, M. Agnew, J. Leach, F. S. Roux, M. J. Padgett, R. W. Boyd, and A. Forbes, "Entangled Bessel-Gaussian beams," Opt. Express **20**, 23589–23597 (2012).
19. W. P. Putnam, D. N. Schimpf, G. Abram, and F. X. Kärtner, "Bessel-Gauss beam enhancement cavities for high-intensity applications," Opt. Express **20**, 24429–24443 (2012).
20. J. W. Goodman, *Introduction to Fourier Optics* (McGraw-Hill, 1966).